

The temperature of hot gas in galaxies and clusters: baryons dancing to the tune of dark matter

Steen H. Hansen¹, Andrea V. Macció², Emilio Romano-Díaz³, Yehuda Hoffman⁴, Marcus Brüggen⁵, Evan Scannapieco⁶, and Greg S. Stinson⁷

¹ *Dark Cosmology Centre, Niels Bohr Institute, University of Copenhagen,
Juliane Maries Vej 30, 2100 Copenhagen, Denmark*

² *Max-Planck-Institut für Astronomie, Königstuhl 17, 69117 Heidelberg, Germany*

³ *Department of Physics & Astronomy, University of Kentucky, Lexington, KY 40506, USA*

⁴ *Racah Institute of Physics, Hebrew University, Jerusalem 91904, Israel*

⁵ *Jacobs University Bremen, P.O. Box 750 561, 28725 Bremen, Germany*

⁶ *School of Earth and Space Exploration, Arizona State University, P.O. Box 871404, Tempe, AZ,
85287-1404, USA*

⁷ *Jeremiah Horrocks Institute, University of Central Lancashire, Preston PR1 2HE*

ABSTRACT

The temperature profile of hot gas in galaxies and galaxy clusters is largely determined by the depth of the total gravitational potential and thereby by the dark matter (DM) distribution. We use high-resolution hydrodynamical simulations of galaxy formation to derive a surprisingly simple relation between the gas temperature and DM properties. We show that this relation holds not just for galaxy clusters but also for equilibrated and relaxed galaxies at radii beyond the central stellar-dominated region of typically a few kpc. It is then clarified how a measurement of the temperature and density of the hot gas component can lead to an indirect measurement of the DM velocity anisotropy in galaxies. We also study the temperature relation for galaxy clusters in the presence of self-regulated, recurrent active galactic nuclei (AGN), and demonstrate that this temperature relation even holds outside the inner region of ≈ 30 kpc in clusters with an active AGN.

Subject headings:

1. Introduction

Dark matter (DM) dominated cosmological structures are a direct outcome of hierarchical structure formation with a subdominant baryon fraction. The baryons can either cool fast to form stars or end up as a hot virialized gas (Rees & Ostriker 1977; Silk 1977; Birnboim & Dekel 2003; Kereš et al. 2005). This hot gas is customarily observed in galaxies and galaxy clusters (Sarazin 1986), and can be heated through adiabatic compression, shock heating or non-gravitational processes and cooled through radiative processes.

The ability of the hot gas to shock heat to the

virial temperature opens the possibility that one can combine the equations governing the dynamics of the gas and the DM, namely the equation of hydrostatic equilibrium and the Jeans equation. The simultaneous solution to these equations can in principle allow us to determine the DM velocity dispersion anisotropy, which holds information about the fundamental difference in the way DM and baryons equilibrate in cosmological structures. In fact, such a method has already been applied to galaxy clusters, where numerical simulations of cluster formation and evolution have been used to confirm that the gas equilibrium temperature is determined through the averaged velocity dispersion of the DM (Hansen & Piffaretti 2007;

Host et al. 2009). The resolution of these simulations, however, did not allow us to probe radii smaller than a few hundred kpc. The temperature of the cooling gas remains to be determined at smaller radii and in the presence of an active AGN. Furthermore, it remains unknown if the gas temperature in galaxies will obey a similar simple relation.

In this paper we conduct a dedicated comparison between the gas and DM in a range of simulated cosmological objects. The structure of the paper is as follows: first we discuss the relationship between the gas temperature and the DM velocity dispersion. In section 3 we present the results of numerical simulations of galaxy formation, and confirm that the gas temperature in galaxies exhibits a bimodal distribution — the hot gas resides at the DM temperature and the cold gas cools below 10^4 K and forms stars. In section 4 we present the results of numerical simulations of AGN outflows, which demonstrate that even when the gas is heated episodically by a self-regulated AGN, it still moves towards the DM temperature, which it succeeds in reaching already beyond ≈ 30 kpc. Finally, in section 5 we explain how our findings open up for the possibility of measuring the DM velocity anisotropy in galaxies, and in section 6 we briefly offer our conclusions.

2. The temperature relation

It has been known for years that baryons in a DM-dominated potential will heat up to a temperature that is determined by the properties of the DM mass profile (Rees & Ostriker 1977; Cavaliere & Fusco-Femiano 1978, 1981; Sarazin 1986; Cavaliere et al. 2009)¹. This is easily seen when considering the similarity between the equation of hydrostatic equilibrium (Sarazin 1986) and the Jeans equation (Binney & Tremaine 1987). The former depends on the gas temperature, T , and through its equation of state on the density, ρ_{gas} , while the latter depends on the DM density, ρ_{DM} , its radial and tangential velocity dispersions,

$\sigma_{r,t}^2$, and the velocity anisotropy $\beta = 1 - \sigma_t^2/\sigma_r^2$,

$$\frac{GM_{\text{tot}}}{r} = -\frac{Tk_B}{\mu m_p} \left[\frac{d \log \rho_{\text{gas}}}{d \log r} + \frac{d \log T}{d \log r} \right] \quad (1)$$

$$\frac{GM_{\text{tot}}}{r} = -\sigma_r^2 \left[\frac{d \log \rho_{\text{DM}}}{d \log r} + \frac{d \log \sigma_r^2}{d \log r} + 2\beta \right] \quad (2)$$

where μm_p is the averaged mass of the gas particles. For a given total mass profile, the hydrostatic equilibrium equation, eq. (1), has a wide range of possible solutions: basically any radial gas temperature profile is allowed (in principle), since a gas density profile can always be constructed to fulfill the equation. Furthermore, there is a priori no theoretical connection between the gas temperature and the dark matter dispersions, except that the particles are sitting in the same gravitational potential. One can, however, use the dark matter dispersions to define a “DM temperature” by

$$\frac{T_{\text{DM}} k_B}{\mu m_p} \equiv \frac{1}{3} (\sigma_r^2 + \sigma_\theta^2 + \sigma_\phi^2), \quad (3)$$

where σ_θ and σ_ϕ are the DM tangential dispersion velocities. We emphasize that there is no fundamental reason why the temperature of the gas, T , should be identical to the DM temperature (in praxis the DM only sets an upper limit to the gas temperature). We will, however, consider the ratio between the gas temperature, and the temperature derived from the DM dispersions, namely

$$\kappa(r) \equiv \frac{T k_B}{\mu m_p} \frac{3}{\sigma_r^2 + \sigma_\theta^2 + \sigma_\phi^2}, \quad (4)$$

and we will discuss a possible universality of this ratio. There is, to our knowledge, no simple dynamical argument why this ratio should be close to unity, or why it should have a universal radial behaviour. For instance, in the adiabatic simulations presented in Faltenbacher et al. (2007) it was found that κ decreases with radius in the inner region. We will here address this question using galaxy formation including cooling, heating and feedback.

Naturally, gravity does not care about the masses of the individual (collisionless) particles, which is why their velocity dispersions are equal, and not their temperatures. The standard definition of the temperature is written in terms of the average kinetic energy of particles and describes a

¹The corresponding stellar velocity dispersion will also be of the same magnitude as the DM velocity dispersion. However, there are no theoretical reason why the anisotropies of the galaxies should be the same as that of the DM (Lokas & Mamon 2003; Wojtak et al. 2009).

system in thermodynamic equilibrium. This thermodynamic limit is not achieved for most particle systems with long-range forces such as gravitational structures, for which this steady state is normally not described by simple distribution functions, e.g., Maxwell-Boltzmann statistics. Thus, the DM is not in thermal equilibrium, and technically it does not have a “temperature”, however, the use of this word should not cause any confusion.

An important point is that the DM temperature, as defined in eq. (3), is not only a function of the mass profile or potential of the DM, but also depends on the dynamical state of the DM through its velocity anisotropy, $\beta(r)$. The velocity anisotropy is much harder to observationally determine than the mass profile. Hence for a nonvanishing velocity dispersion anisotropy in the DM, the DM temperature is not identical to the velocity dispersion of the DM along any random direction, such as the radial direction, but only to their spatial average.

We will now proceed to analyse the ratio between the local gas and DM temperatures defined in eq.(4), and use numerical simulations of galaxy clusters or galaxies to test if κ is of order unity. Considering the results of two different numerical codes (Kay et al. 2007; Valdarnini 2006) simulating both DM and baryonic physics, Host et al. (2009) demonstrated that the $\kappa = 1$ within 20% for relaxed galaxy clusters. The gas in galaxies is much denser, and the cooling times are, therefore, much shorter, and one might have expected that κ might have a much more complicated profile. We demonstrate below that indeed the hot gas in galaxies does have virtually universal temperature ratios, with $\kappa \approx 1$.

3. Numerical simulations

The hydrodynamical simulations were performed with GASOLINE (Wadsley et al. 2004; see Governato et al. (2007) or Stinson et al. (2010) for a more detailed description) — multi-stepping, parallel TreeSPH N -body code. We include radiative and Compton cooling for a primordial mixture of hydrogen and helium. The star formation algorithm is based on a Jeans instability criteria (Katz 1992), where gas particles in dense, unstable regions and in convergent flows spawn star particles

at a rate proportional to the local dynamical time (see Governato et al. 2004). The star formation efficiency was set to 0.05, but in the adopted scheme its precise value has only a minor effect on the star formation rate (Katz 1992). The code also includes supernova feedback (Stinton et al. 2006), and a UV background (Haardt & Madau 1996; Heller 1999). Additional simulations using the FTM 4.5 code (Heller & Shlosman 1994) are described in Section 3.1.

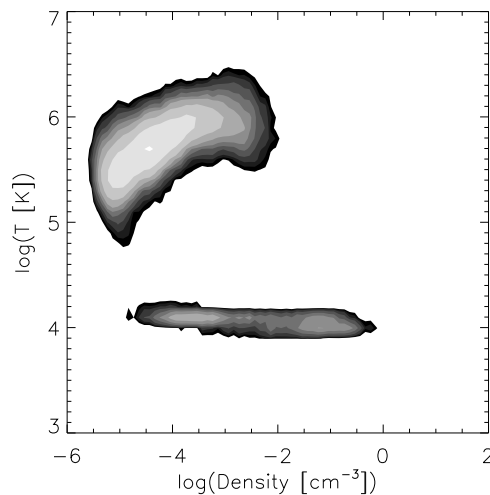


Fig. 1.— Contour plot of the gas density and temperature of the individual gas particle at $z = 0$ from the numerical simulation using GASOLINE of the galaxy G2. The gas particles either cool down to the floor of the atomic cooling 10^4 K, or stay at the DM temperature around 10^6 K.

For the simulations with GASOLINE, we selected three candidate haloes with masses similar to the mass of the Milky Way ($M \approx 10^{12} M_\odot$) from an existing low-resolution DM simulation (300^3 particles within 90 Mpc) and re-simulated them at higher resolution. These high-resolution runs are 8^3 times more resolved in mass than the initial ones and included a gaseous component within the entire high-resolution region. In these runs the masses of the DM and gas particles are respectively $m_d = 1.17 \times 10^6 h^{-1} M_\odot$ and $m_g = 2.3 \times 10^5 h^{-1} M_\odot$. The DM has a spline gravitational softening length of $500 h^{-1}$ pc and there are about 10^6 particles for each component (dark and

gas) in the high-resolution region. More properties of the galaxies are listed in Table 1. These hydrodynamical simulations are described in details in Schewtschenko & Macciò (2010).

Table 1: Galaxies parameters

Galaxy	Mass ($10^{12} h^{-1} M_{\odot}$)	R_{vir} (kpc h^{-1})	V_{circ} (km s $^{-1}$)
G0	0.74	188	178
G1	0.89	199	188
G2	0.93	202	203

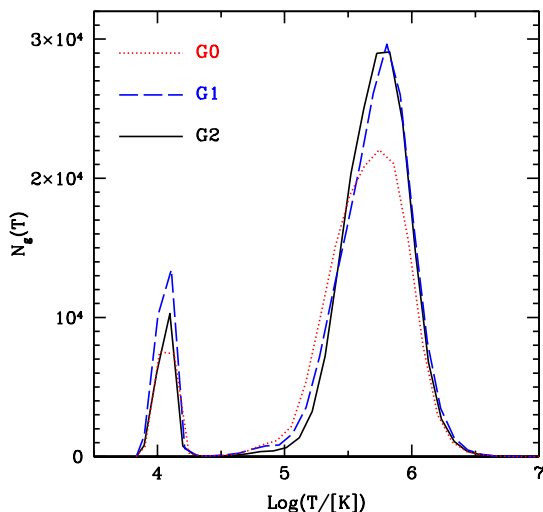


Fig. 2.— Histogram of the individual gas particle temperatures at $z = 0$ from the numerical simulation using GASOLINE. The three curves represent each of the three galaxies simulated at high resolution. The gas particles either cool down to the floor of the atomic cooling 10^4 K, or stay at the DM temperature around 10^6 K.

In Fig. 1 we show contours over the temperature and local density of all the gas particles in one of the 3 galaxies (the others look essentially identical). In Fig. 2 we show histograms over the individual gas particle temperatures in the three selected galaxies, which is a projection of figure 1. The gas temperature exhibits a bimodal distribution: it either cools down to the floor of atomic cooling about 10^4 K in dense clumps (central disk/bulge or satellite cores) or stays at

the DM temperature in the larger and less dense regions. This is largely caused by the significantly shorter cooling time around 10^5 K (see e.g. Kereš et al. (2005)). When we discuss the gas temperature from the simulations using GASOLINE we refer to the second (large) bump. Practically we calculate a mass-averaged temperature by including only particles warmer than $10^{4.5}$ K. Making a mass-average over all particles (including the cold ones) makes a negligible difference at most times. There is no metal cooling in this simulation, which is the reason for the floor at 10^4 K. The galaxies are typical field galaxies, and have been selected to have a quiet merger history (except G1, which had a major merger at $z = 0.8$).

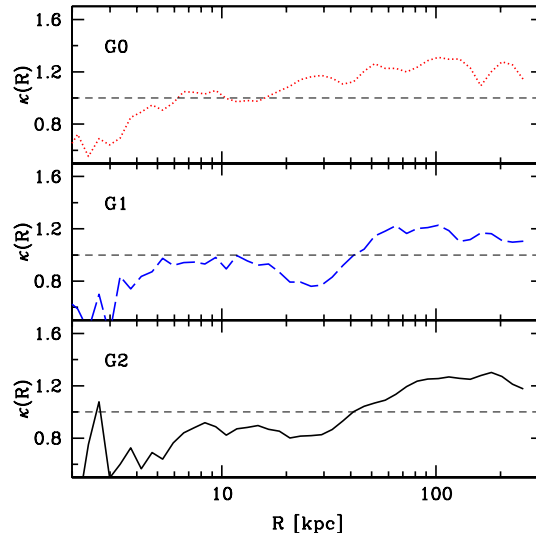


Fig. 3.— The temperature ratios as a function of radius for the three simulated galaxies. The frames show that outside the central region of ≈ 6 kpc where the stellar disk dominates the potential, the ratio, $\kappa(r) = \sigma_{\text{baryons}}^2 / \langle \sigma_{\text{DM}}^2 \rangle$ approaches unity.

We can now consider radial bins for each galaxy at $z = 0$, and in each bin we calculate the mass-averaged gas temperature and the mass-averaged DM velocity dispersion. Their ratios as in eq.(4) is shown in Fig. 3. From this figure we see that outside the range of the disk, i.e. beyond ≈ 6 kpc, these ratios remain close to unity. Beyond 20 kpc, where the gas density is lower and hence the cooling time longer, the gas temperature is slightly

above the DM dispersion velocities by 10%–20%. The velocity anisotropy is nearly constant, $\beta(r) \approx 0.2$ outside 2 kpc, slowly increasing to about 0.3 near 100 kpc. We thus confirm that indeed there remains a substantial component of the hot gas at the DM temperatures even in dense environments of galaxies.

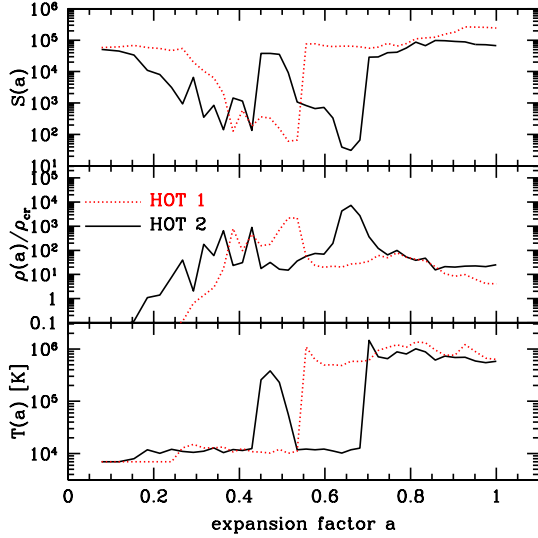


Fig. 4.— History of 2 hot gas particles. Shown is entropy, local density, and temperature as function of expansion factor.

3.1. History of hot and cold particles

In order to better understand the origin of the above bimodal distribution of gas temperatures, we tracked the evolution of various properties of individual particles. Each gas particle has its own unique thermal history, however, it appears that we as a first approximation can split the particles into four groups.

- 1) Hot particles, which are shock heated to roughly 10^6 K, and then keep that temperature.
- 2) Warm particles, which are shock heated to roughly 10^6 K, and then slowly cooled down somewhat. These constitute less than 15% of the particles with $T > 10^{4.5}$ K.
- 3) Cold particles close to the centre ($r < 15$ kpc). These are shock heated, and then they

cooled down very quickly. These may have experience several episodes of heating and cooling.

- 4) Cold particles which are never shock heated. These particles come through the cold accretion phase.

The two cold modes (3 and 4 above) were discussed in detail in Kereš et al. (2005); Macciò et al. (2006).

In Figs. (4,5) we present the entropy, local density near the particle, and temperature as function of the expansion factor. In Fig. 4 we present the history of 2 particles which are hot today. The first particle (Hot 1) only has one period of heating as it enters the final halo. The second gas particle (Hot 2) has one episode of heating followed by rapid cooling in its first subhalo, followed by heating when it enters the final halo. In Fig. 5 we present the history of two particle which are cold today. The first (Cold 1) has been accreted cold, and it never experienced any shock heating. The second particle (Cold 2) had 2 periods of heating followed by rapid cooling, which is clearly seen to happen when the particle enters the high density region.

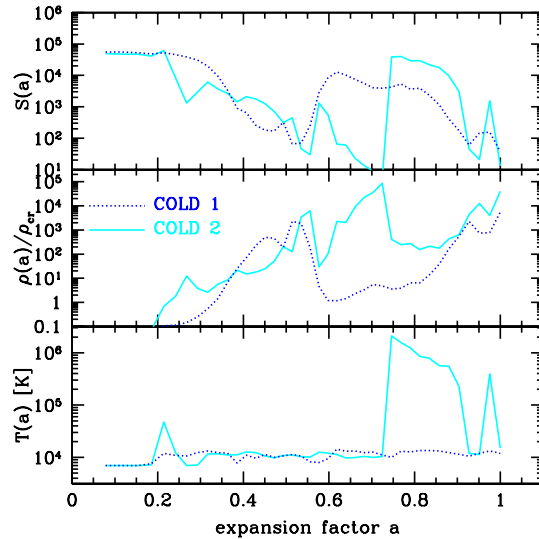


Fig. 5.— History of 2 cold gas particles. Shown is entropy, local density, and temperature as function of expansion factor.

3.2. Evolution of κ with redshift

In order to test the generality of the above results, that $\kappa(r) \approx 1$, we present results from independent simulations of Romano-Díaz et al. (2008a,b, 2009) using the parallel version of the hybrid SPH/ N -body FTM 4.5 code (Heller & Shlosman 1994; Heller, Shlosman & Athanasoulas 2007). The gravitational forces are computed using the falcON routine (Dehnen 2002) which scales as $O(N)$. The tolerance parameter θ is fixed at 0.55. The gravitational softening applied is $\epsilon = 500$ pc for the DM, stars, and gas. The vacuum boundary conditions are used and the simulations are performed with physical coordinates. The cosmological constant is introduced by an explicit term in the acceleration equation. The conservation of the total angular momentum and energy within the computational sphere in the collisionless models is within $\sim 0.01\%$ and $\sim 1\%$, respectively. The evolution of various parameters characterizing the DM and baryons is followed in 1000 snapshots, linearly spaced in the cosmological expansion parameter a .

The modeling of star formation (SF) processes and associated feedback are described in Heller & Shlosman (1994) and Heller et al. (2007), which should be consulted for details. Feedback from OB stellar winds and supernovae (SN) Type II is also included. A fraction of this energy is thermalized and deposited in the gas in the form of thermal energy, then converted to kinetic energy through the equations of motion. This method is preferable over injecting a fraction of the stellar energy directly in the form of a kinetic energy (Heller et al. 2007).

Multiple generations of stars are allowed to form from each gas particle. The evolution of gas metallicity is followed and the fraction of massive stars that lead to the OB stellar winds and SN is calculated from the Salpeter IMF.

Fig. 6 displays the redshift evolution of the radial profiles of the temperature ratio, κ . All the gas particles (both hot and cold) are included in the averages here, and therefore different aspects of the time evolution of $\kappa(r)$ can be followed. At higher redshifts, $z \geq 2$, when the disk is being assembled from the cold gas supplied by the filaments, and which is converted into stars, the temperature ratio drops below unity in the disk re-

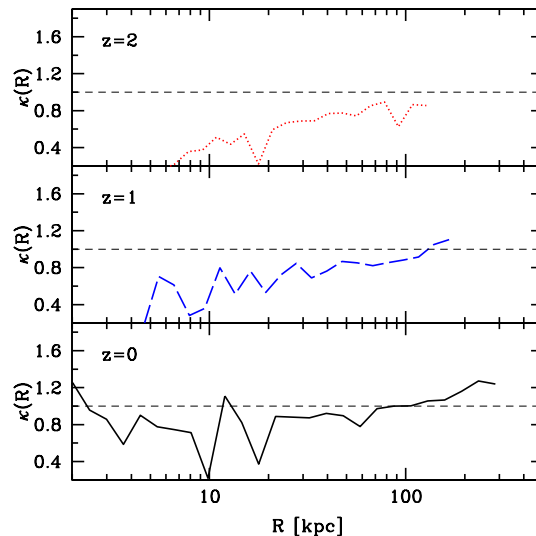


Fig. 6.— Evolution of $\kappa(r)$ with redshift using cosmological simulations of galaxy formation and evolution by Romano-Díaz et al. (2009). From top to bottom the frames show $\kappa(r)$ at redshifts $z = 2, 1, 0$.

gion. For $z < 1$, when the star formation, feedback by SN and stellar winds (Romano-Díaz et al. 2008b, 2009) consume a large fraction of this gas, the temperature ratio rises to unity, as the heated gas tends to the DM temperature. After $z \approx 1$ we observe an influx of subhalos along the filaments which ablate the cold gas from the disk nearly completely. Two independent parameters verify the overall evolution of the model from a late-type to the early-type: the fraction of the gas-to-disk mass ratio, and the ratio of a spheroidal-to-disk mass ratio (within the disk radius). At $z = 0$ we find a temperature ratio which is slightly below unity in the central region, and rises to slightly above unity towards the virial radius.

Hence, we see that the gas-to-DM temperature ratio approaches unity for the evolved and relaxed galaxies. Of course, the actual evolution of the ratio does depend on the particular history of the galaxy, but the important point here is, that for equilibrated galaxies today, the temperature ratio is close to unity.

As a sidenote we point out that the stellar dispersion does not agree with the DM dispersion for these galaxies. We can therefore not use the stellar

velocities in the same way to extract information about the DM, and we cannot assume that the stellar velocity dispersion anisotropy should equal that of the DM.

4. AGN outflows

The simple relation between the gas and DM velocity dispersions in eq. (3) has been demonstrated using numerical simulations for galaxy clusters in Host et al. (2009). Those simulations had sufficient resolution to probe a region outside of roughly 100-200 kpc. It remains unknown if this simple relation still holds further towards the central region, where cooling may be faster, or where a central AGN may pump energy into the intra-cluster gas.

To address this question, we present results of a simulation of a three-dimensional model of AGN self-regulation in a cool-core cluster (Brüggen & Scannapieco 2009). This simulation was performed with FLASH version 3.0 (Fryxell et al. 2000) a multidimensional adaptive mesh refinement hydrodynamics code, which solves the Riemann problem on a Cartesian grid using a directionally-split Piecewise-Parabolic Method (PPM) solver. In this simulation the cluster properties, such as the density and temperature profiles have been chosen to resemble the best-studied cluster, the Perseus cluster. The gravitational potential is taken to be static, and initially the gas is set up in hydrostatic equilibrium. The gas physics includes radiative cooling, heating through AGN feedback and a subgrid model for Rayleigh-Taylor-driven turbulence, as described in Brüggen & Scannapieco (2009). Unlike in previous simulations, the energy input rate was not predetermined, but instead calculated from the instantaneous conditions near the centre of the cluster. A fixed fraction of the mc^2 rest mass energy of the accreted gas is returned to the ICM in the form of AGN-blown cavities whose turbulent evolution couples them to the inflowing cool gas (Brüggen et al. 2009). When turbulence is properly accounted for, the model results in a self-regulated AGN, where a phase of an episodic heating is followed by a quiescent phase, where the cool-core reforms.

For a wide range of feedback efficiencies, the cluster regulates itself for at least several 10^9 years.

Heating balances cooling through a string of outbursts with typical recurrence times of around 80 Myrs, a timescale that depends on global cluster properties.

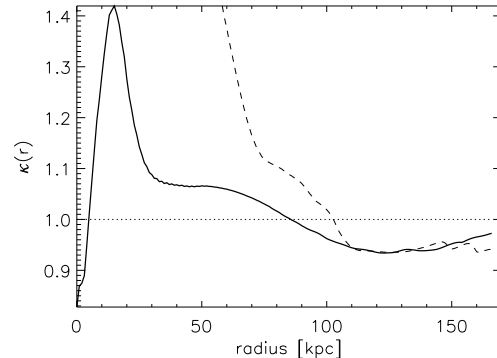


Fig. 7.— The temperature ratio as function of radius for the simulated galaxy cluster with a recurrent AGN heating source. The full line shows the temperature ratio of the fiducial run of a self-regulating AGN in a cool core cluster after 1 Gyr, labeled D5-10 in Brüggen & Scannapieco (2009). This figure demonstrates that outside the central region (≈ 30 kpc, where the recent AGN burst has heated the gas temperature much above the DM temperature) the ratio $\kappa(r) = \sigma_{\text{baryons}}^2 / \langle \sigma_{\text{DM}}^2 \rangle$ is unity, within 10%. The dashed line shows the results from an extreme case of AGN-feedback, where strong outflows occur every 50 Myrs (Scannapieco & Brüggen 2008).

In Fig. (7) we see that for the self-regulating AGN feedback model after 1 Gyr (solid line), the spherically averaged gas dispersion does indeed agree with the DM dispersion within 10%, at radii larger than 30 kpc. This case represents the best available simulation of a self-regulating cool core cluster which reproduces a number of key features seen in X-ray observations (Brüggen & Scannapieco 2009).

In the central region, at radii smaller than 30 kpc, we see a sharp increase in the gas temperature resulting from a recent AGN burst, and at the very centre, within less than 10 kpc, we observe the effect of very rapid gas cooling, and the re-emergence of a cool core.

To test an extreme case of AGN heating of a cluster core, we also present the results from a

model where AGN-driven bubbles occur at regular intervals of 50 Myrs with bubble energies of 5×10^{59} ergs (Scannapieco & Brüggen 2008). Even for this non-self regulated, and somewhat less physically motivated case, the dashed line in Fig. (7) shows that, as long as we consider radii outside of 70–100 kpc region, the velocity dispersion ratio stays within 10% of unity.

5. Implications for the velocity anisotropy

For the self-regulated AGN, the simple temperature relation $\kappa(r) \approx 1$ holds outside the inner region of $r \approx 30$ kpc, as we have shown in section 4. For the observed X-ray clusters studied in Host et al. (2009), this radius corresponds roughly to the centre of the innermost bin. This shows that one can trust the inference of the DM velocity anisotropy in galaxy clusters down to radii as small as ≈ 50 kpc.

In the case of galaxies, we have demonstrated that the simple temperature relation holds for relaxed and equilibrated structures, when applied to radii beyond the regions dominated by the stellar component. This opens for the possibility of indirectly determining the DM velocity anisotropy in galaxies in the following way. By measuring the temperature and the density of the hot X-ray emitting gas, one may use the equation of hydrostatic equilibrium, eq. (1), to measure the total gravitating mass. Now, considering the Jeans equation, eq. (2), we see that it contains the total mass on the left hand side, and 3 unknown quantities on the right hand side ($\rho_{DM}, \sigma_r^2, \beta$). First, combining the total mass measurement from X-ray with spectral determination of the stellar mass, allows one to determine the DM density profile

$$\rho_{DM}(r) = f_1(T_g(r), \rho_g(r), \rho_{star}(r)) . \quad (5)$$

We are thus left with 2 unknowns on the right hand side of the Jeans equation, eq. (2), namely the radial dispersion and the velocity anisotropy, β . Using the temperature relation, eq. (3), together with the X-ray determined gas temperature, we get rid of one of these, and hence get an indirect measurement of the dark matter velocity anisotropy

$$\beta(r) = f_2(\kappa(r), T_g(r), \rho_g(r), \rho_{star}(r)) . \quad (6)$$

Such observation has only very recently become possible for X-ray bright galaxy clus-

ter (Hansen & Piffaretti 2007; Morandi & Ettori 2007; Host et al. 2009), and it is clear that such indirect observations in galaxies most likely will require improved X-ray satellites. The simplest possibility would be if $\kappa(r) = 1$ everywhere, however, the method to infer the DM velocity anisotropy as described above, works as long as the radial form of $\kappa(r)$ is known (Host et al. 2009). This is exactly one of the points of this paper, that the form of $\kappa(r)$ appears to be universal for galaxies (see figure 3).

A direct measurement of this velocity anisotropy is expected to be virtually impossible in terrestrial experiments (Host & Hansen 2007). Measuring β of the DM in galaxies, as described above, can provide an independent confirmation to virtually every numerical modeling of DM halo formation in the cosmological context, and to the suggestion that a non-zero β is a fundamental property of galactic DM halos, even in equilibrium (Hansen 2009; Hansen et al. 2010). Furthermore, a non-zero β has an effect on the underground direct detection experiments (Vergados 2000; Evans et al. 2000; Vergados et al. 2008). A detection through the method laid out above would therefore decrease the systematic error-bars in terrestrial DM detection experiments.

6. Conclusions

In summary, we have found a very simple relation between the temperature of the hot gas and the averaged dispersion of the dark matter, namely that their ratio is close to unity, $\kappa \approx 1$. We have demonstrated that this near equality of the gas and DM temperatures holds in the case of equilibrated and relaxed galaxies.

This relation is not only conceptually important, but it will also allow an indirect determination of the dark matter velocity anisotropy in galaxies. Such an observation will provide an important and independent confirmation of all cosmological DM halo formation simulations.

We have also studied this relation in galaxy clusters containing an active AGN, and our results confirm that one can indeed use galaxy clusters to infer the dark matter velocity anisotropy.

It is a pleasure to thank Isaac Shlosman for insightful discussions. SHH thanks Ole Host, Marco Roncadelli and Darach Watson for discussions. Numerical simulations were performed on the PIA and on the PanStarrs2 clusters of the Max-Planck-Institut für Astronomie at the Rechenzentrum in Garching and on the zBox2 supercomputer at the University of Zürich. Special thanks to B. Moore, D. Potter and J. Stadel for bringing zBox2 to life. E.R.D. simulations have been run on a dedicated cluster. The AGN simulations were conducted on the "Saguaro" cluster operated by the Fulton School of Engineering at Arizona State University. Y.H. has been partially supported by the ISF (13/08). The Dark Cosmology Centre is funded by the Danish National Research Foundation.

REFERENCES

- Binney, J., & Tremaine, S. 1987, Princeton, NJ, Princeton University Press, 1987, 747 p.
- Birnboim, Y., & Dekel, A. 2003, MNRAS, 345, 349
- Brüggen, M., & Scannapieco, E. 2009, MNRAS, 398, 548
- Brüggen, M., Scannapieco, E., & Heinz, S. 2009, MNRAS, 395, 2210
- Cavaliere, A., & Fusco-Femiano, R. 1978, A&A, 70, 677
- Cavaliere, A., & Fusco-Femiano, R. 1981, A&A, 100, 194
- Cavaliere, A., Lapi, A., & Fusco-Femiano, R. 2009, ApJ, 698, 580
- Dehnen, W. 2002, J. Comput. Phys., 179, 27
- Evans, N. W., Carollo, C. M., & de Zeeuw, P. T. 2000, MNRAS, 318, 1131
- Fabian, A. C., Nulsen, P. E. J., & Canizares, C. R. 1991, A&A Rev., 2, 191
- Faltenbacher, A., Hoffman, Y., Gottlöber, S., & Yepes, G. 2007, MNRAS, 376, 1327
- Fryxell, B., et al. 2000, ApJS, 131, 273
- Governato, F., et al. 2004, ApJ, 607, 688
- Governato, F., Willman, B., Mayer, L., Brooks, A., Stinson, G., Valenzuela, O., Wadsley, J., & Quinn, T. 2007, MNRAS, 374, 1479
- Haardt, F., & Madau, P. 1996, ApJ, 461, 20
- Hansen, S. H., & Piffaretti, R. 2007, A&A, 476, L37
- Hansen, S. H. 2009, ApJ, 694, 1250
- Hansen, S. H., Juncker, D., & Sparre, M. 2010, ApJ, 718, L68
- Heller, C. H., & Shlosman, I. 1994, ApJ, 424, 84
- Heller, C. H., Shlosman, I., & Athanassoula, E. 2007, ApJ, 671, 226
- Host, O., & Hansen, S. H. 2007, JCAP, 0706, 016
- Host, O., Hansen, S. H., Piffaretti, R., Morandi, A., Ettori, S., Kay, S. T., & Valdarnini, R. 2009, ApJ to appear, arXiv:0808.2049
- Kay, S. T., da Silva, A. C., Aghanim, N., Blanchard, A., Liddle, A. R., Puget, J.-L., Sadat, R., & Thomas, P. A. 2007, MNRAS, 377, 317
- Katz, N. 1992, ApJ, 391, 502
- Kereš, D., Katz, N., Weinberg, D. H., & Davé, R. 2005, MNRAS, 363, 2
- Lokas, E. L., & Mamon, G. A. 2003, MNRAS, 343, 401
- Macciò, A. V., Moore, B., & Stadel, J. 2006, ApJ, 636, L25
- Mo, H. J., & White, S. D. M. 2002, MNRAS, 336, 112
- Morandi, A., & Ettori, S. 2007, MNRAS, 380, 1521
- Rees, M. J., & Ostriker, J. P. 1977, MNRAS, 179, 541
- Romano-Díaz, E., Shlosman, I., Heller, C., & Hoffman, Y. 2009, ApJ, 702, 1250
- Romano-Díaz, E., Shlosman, I., Hoffman, Y., & Heller, C. 2008a, ApJ, 685, L105
- Romano-Díaz, E., Shlosman, I., Heller, C. & Hoffman, Y. 2008b, ApJ, 685, L13

- Sarazin, C. L. 1986, *Reviews of Modern Physics*, 58, 1
- Scannapieco, E., & Brüggen, M. 2008, *ApJ*, 686, 927
- Schewtschenko, J., & Macciò, A. 2010, *MNRAS*, in press, arXiv:1012.0311
- Silk, J. 1977, *ApJ*, 211, 638
- Stinson, G., Seth, A., Katz, N., Wadsley, J., Governato, F., & Quinn, T. 2006, *MNRAS*, 373, 1074
- Stinson, G. S., Bailin, J., Couchman, H., Wadsley, J., Shen, S., Nickerson, S., Brook, C., & Quinn, T. 2010, *MNRAS*, 408, 812
- Valdarnini, R. 2006, *New Astronomy*, 12, 71
- Vergados, J. D. 2000, *Phys. Rev. D*, 62, 023519
- Vergados, J. D., Hansen, S. H., & Host, O. 2008, *Phys. Rev. D*, 77, 023509
- Wadsley, J. W., Stadel, J., & Quinn, T. 2004, *New Astronomy*, 9, 137
- Wojtak, R., Łokas, E. L., Mamon, G. A., & Gottlöber, S. 2009, *MNRAS*, 399, 812